to appear in ApJ

Herschel Observations of Far-Infrared Cooling Lines in intermediate Redshift (Ultra)-luminous Infrared Galaxies*

D. Rigopoulou[1,2], R. Hopwood[3], G.E. Magdis[1], N. Thatte[1], B.M. Swinyard[2,4] D. Farrah[5], J-S. Huang[6], A. Alonso-Herrero[7], J.J. Bock[8,9], D. Clements[3], A. Cooray[10,9], M.J. Griffin[11], S. Oliver[12], C. Pearson[2,13], D. Riechers[14], D. Scott[15] A. Smith[12], M. Vaccari[16], I. Valtchanov[17], L. Wang[12]

ABSTRACT

[1]Department of Physics, University of Oxford, Keble Road, Oxford, OX1 3RH, UK

[2]RAL Space, Science & Technology Facilities Council, Rutherford Appleton Laboratory, Didcot, OX11 0QX, UK

[3]Physics Department, Imperial College London, South Kensington Campus, London SW7 2AZ, UK

[4]Dept. of Physics & Astronomy, University College London, Gower St, London, WC1E 6BT, UK

[5]Department of Physics, Virginia Tech, Blacksburg, VA 24061, USA

[6]Harvard-Smithsonian Center for Astrophysics, 60 Garden Str., Cambridge, MA02138, USA

[7]Instituto de Fisica de Cantabria, CSIC-UC, 39006 Santander, Spain

[8]California Institute of Technology, 1200 E. California Blvd., Pasadena, CA 91125, USA

[9]Jet Propulsion Laboratory, 4800 Oak Grove Drive, Pasadena, CA 91109, USA

[10]Department of Physics & Astronomy, University of California, Irvine, CA 92697, USA

[11]School of Physics and Astronomy, Cardiff University, Queens Buildings, The Parade, Cardiff CF24 3AA, UK

[12]Astronomy Centre, Department of Physics & Astronomy, University of Sussex, Brighton BN1 9QH, UK

[13]Department of Physical Sciences, The Open University, Milton Keynes MK7 6AA, UK

[14]Department of Astronomy, Cornell University, 220 Space Sciences Building, Ithaca, NY 14853, USA

[15]Department of Physics and Astronomy, University of British Columbia, 6224 Agricultural Road, Vancouver, B.C. V6T1Z1, Canada

[16]Astrophysics Group, Physics Department, University of the Western Cape, Private Bag X17, 7535 Bellville, Cape Town, South Africa

[17]Herschel Science Centre, European Space Astronomy Centre, Villanueva de la Canada, E-28691 Madrid, Spain

We report the first results from a spectroscopic survey of the [CII] 158μm line from a sample of intermediate redshift (0.2< z <0.8) (ultra)-luminous infrared galaxies, (U)LIRGs (L_{IR} >$10^{11.5}L_{\odot}$), using the SPIRE-Fourier Transform Spectrometer (FTS) on board the *Herschel* Space Observatory. This is the first survey of [CII] emission, an important tracer of star-formation, at a redshift range where the star-formation rate density of the Universe increases rapidly. We detect strong [CII] 158μm line emission from over 80% of the sample. We find that the [CII] line is luminous, in the range (0.8−4)×10^{-3} of the far-infrared continuum luminosity of our sources, and appears to arise from photodissociation regions on the surface of molecular clouds. The $L_{[CII]}/L_{IR}$ ratio in our intermediate redshift (U)LIRGs is on average ∼10 times larger than that of local ULIRGs. Furthermore, we find that the $L_{[CII]}/L_{IR}$ and $L_{[CII]}/L_{CO(1-0)}$ ratios in our sample are similar to those of local normal galaxies and high-z star-forming galaxies. ULIRGs at $z \sim 0.5$ show many similarities to the properties of local normal and high-z star forming galaxies. Our findings strongly suggest that rapid evolution in the properties of the star forming regions of luminous infrared galaxies is likely to have occurred in the last 5 billion years.

Subject headings: infrared: galaxies — infrared: ISM — galaxies: starburst

1. Introduction

Luminous ($10^{11} < L_{IR(8-1000)}<10^{12}$ $L_{\odot}$) and ultra-luminous IR galaxies ($L_{IR(8-1000)}$ >10^{12} $L_{\odot}$, (U)LIRGs) are amongst the most important populations in studies of galaxy evolution. The origin of their extreme luminosities has been the focus of debate since their discovery by IRAS however, it is now widely accepted that local (z<0.26) ULIRGs are primarily powered by star-formation (e.g. Genzel et al. 1998, Rigopoulou et al. 1999, Farrah et al. 2007).

While ULIRGs in the local Universe are rare (e.g. Lagache et al. 2005), they contribute significantly to the total IR energy density from redshifts 0.5 and above (e.g. Le Floc'h et al. 2005, Rodighiero et al. 2010). At redshifts z >2 submillimetre galaxies (SMGs) are considered to be the more luminous counterparts of local ULIRGs (e.g. Blain et al. 2002). There are many indications however, that local ULIRGs differ systematically from their high redshift counterparts. Many authors (e.g. Papovich et al. 2007, Farrah et al. 2008, Muzzin

*Herschel is an ESA space observatory with science instruments provided by European-led Principal Investigator consortia and with important participation from NASA

et al. 2010, Swinbank et al. 2010) have found that high-z ULIRGs have different Spectral Energy Distributions (SEDs), mid-infrared properties and extent of star-forming regions when compared to local ones. More recently, Rujopakarn et al. (2011) compared physical scales of the star-forming regions and concluded that high-z ULIRGs are more akin to local star-forming galaxies rather than local ULIRGs.

The fine structure line [CII] at 158 μm is one of the brightest emission lines in the spectra of galaxies. [CII] traces gas exposed to far-ultraviolet (FUV) photons from OB stars with energies greater than 11.3 eV, the ionisation potential of C^0. In these photodissociation regions (PDRs), atomic, molecular, hydrogen and electrons can collisionally excite the ground state of C^+ ions producing [CII] which cools the gas. Early [CII] detections with the Kuiper Airborne Observatory (KAO) in nearby galaxies showed that the line was bright, 0.1−1% of the observed far-infrared (FIR) luminosity (e.g. Stacey et al. 1991, Crawford et al. 1985). Subsequent observations with the *Infrared Space Observatory (ISO)* confirmed these findings but highlighted a deficit of the [CII] line in the highest luminosity systems such as local ULIRGs (e.g. Luhman et al. 1998, 2003).

Since most local ULIRGs are thought to be star-formation dominated (e.g. Genzel et al. 1998, Rigopoulou et al. 1999) the [CII]-deficit appeared at odds with previous results and a number of explanations were put forward, including size of [CII] emitting regions, metallicity and dust content (e.g. Luhman et al. 1998, 2003). But recent detections of [CII] in luminous z>1.5 star-forming systems with *Herschel* (e.g. Ivison et al. 2010, Valtchanov et al. 2011, George et al. 2013) and other ground-based facilities (e.g. Hailey-Dunsheath et al. 2010, Stacey et al. 2010) revealed that their [CII]/FIR luminosity ratios are similar to local star-forming galaxies, much above the median values found for local ULIRGs. More recently, Gracia-Carpio et al. (2011) found that the [CII]/L_{FIR} ratio is inversely proportional to L_{FIR}/ M(H_2) for a fixed L_{FIR} for a sample of local starbursts and (U)LIRGs.

Here we present the first results of a survey of [CII] in a sample of $0.2<z<0.8$ (U)LIRGs. The redshift range $0.2<z<0.8$ represents a crucial phase in galaxy evolution: it is exactly in this range that the star formation density of the Universe increases steeply, becoming essentially flat at $z>1.5$ (e.g. Magnelli et al. 2013, Bouwens et al. 2009). [CII] observations of galaxies in this cosmic epoch will establish the long-sought link between the local and high-z Universe and allow us to form a benchmark for future studies of [CII] at higher redshifts.

2. Sample Selection & Observations

2.1. The Sample

The primary goal of the survey is to investigate the properties of the ISM and in particular whether intermediate redshift (U)LIRGs are [CII]-deficient like their local counterparts. To construct the present sample we employed the *Herschel* Multi-tiered Extragalactic Survey (HerMES, Oliver et al. 2012) photometric catalogues produced using a prior source extraction based on the position of known 24 μm sources (XID, Roseboom et al. 2012). We searched for sources that satisfied the following two criteria: (1) $S_{250} > 150$ mJy, a limit imposed to ensure detection of the source against the background emission of the telescope at 80 K and, (2) redshift in the range $0.2<z<0.8$ so that we could observe at least one of the primary cooling lines [CII] 158 μm, [NII] 205 μm and [CI] 307 μm in the 194−671 μm range. These criteria resulted in the selection of 22 (U)LIRGs with $L_{\rm IR(8-1000)}>10^{11.2}L_\odot$, 17 of them with confirmed spectroscopic redshifts ($z_{\rm spec}$).

We have supplemented the far-infrared spectroscopic data with single-dish CO data using the IRAM 30 m and ESO APEX telescopes and, spatially resolved optical Integral field spectroscopic data using the Oxford-SWIFT IFU (Thatte et al. 2010) on Palomar. The present Letter focuses on 12 intermediate redshift (U)LIRGs with $z_{\rm spec}$ for which the [CII] 158 μm line falls in the SPIRE-FTS range. We note that the [OI]63 μm line does not fall in the FTS range, hence we assume that [CII] is the primary cooling line in our sample. Measurements of the full sample and reports of the ancillary datasets and measurements will be presented in Magdis et al. (2014).

2.2. SPIRE-FTS Spectroscopy

The (U)LIRGs in our sample were observed with the Spectral and Photometric Imaging REceiver (SPIRE; Griffin et al. 2010) Fourier Transform Spectrometer (FTS) on board the *Herschel* Space Observatory (Pilbratt et al. 2010), between March 2012 and January 2013. The FTS observed 100 repetitions (13320 seconds total integration time) on each target in single pointing, high spectral resolution (0.048 cm^{-1}) mode, with sparse spatial sampling. The SPIRE-FTS measures the Fourier transform of the spectrum of a source using two bolometer detector arrays, simultaneously covering wavelength bands of 194−313 μm (SSW) and 303−671 μm (SLW). All (U)LIRGs in the sample are point-like, given the beam size in SSW and the distances. A typical spectrum around the [CII] line is shown in Fig. 1. All ULIRGs in our sample are extremely faint targets for the FTS and, require post-pipeline processing beyond the standard reduction. A detailed account of the procedure used can be

found in Hopwood et al. (2013). In brief, we used the standard FTS pipeline (Fulton et al. 2013b in prep) in HIPE (Ott et al. 2010) version 11 to reduce the data. Within the pipeline steps, a bespoke Relative Spectral Response Function (RSRF) constructed from selected long dark sky observations was applied if it improved the noise in the point source calibrated product (level-2 product).

Two methods can be used to remove residual background in the level-2 spectra. Firstly, spectra from detectors around the central "on-source" detector were selected and their average spectra subtracted from the central detector. The second method involves subtracting a dark sky spectrum observed on the same operational day. We found the off-axis subtraction provided the best reduction in residual for all but one observation. Once the optimum reduction method was determined and the level-2 spectra obtained, these were examined for spectral features. Since random noise in an FTS spectrum can easily mimic a faint line we used the jackknife technique as a reliability test to minimise spurious detections. In brief, each unaveraged level-2 spectrum, of 200 scans, was split into sequential subsets. This was repeated for subsets of decreasing number of scans. By plotting the averaged subsets at the expected line positions and making a visual comparison over all subsets, an assessment of the presence of an expected line was made.

Once a line was assessed as real, a bootstrap method was used to measure the line flux. For any given observation, scans were randomly sampled until the number in the parent population (of 200) was reached. These random scans were then averaged and the line measurements made by fitting a sinc function, or, if the line was partially resolved (in six cases) we employed a sinc convolved with a Gaussian. We repeated the process 10,000 times for each observation and fitted a Gaussian to the resulting line flux distribution to obtain the mean line flux. The standard deviation was taken as the associated 1σ uncertainties. Random frequency positions were also selected and the same process repeated to give comparison distributions and provide a second reliability check. Due to the nature of FTS random and systematic noise, the distributions obtained for random frequency positions are indistinguishable to those for faint lines ($< 2\,\sigma$), however, a background level can be established with the bootstrapped results for these randomly selected positions, above which a real spectral feature is strongly suggested. For any line found to be below $2\,\sigma$, the bootstrapped flux density is taken as an upper limit, but only if the presence of a [CII] line is supported by the jackknife and other visual checks.

3. Results

3.1. The $L_{[CII]}/L_{IR}$ Relationship

We have detected [CII] line emission ($>3\sigma$) from 10 of the 12 ULIRGs with z_{spec}. The [CII] line is bright in all detected sources, in the range (0.6-2.6)$\times10^9$L$_\odot$. The brightest source, with a [CII] line luminosity of 5.7×10^{10} L$_\odot$ has been identified with a z=2.31 luminous galaxy merger (XMM01, Fu et al. 2013) although the lens galaxy was originally selected. The two sources with the lowest [CII] line luminosity both contain spectroscopically confirmed AGN (Houck et al. 2003) but are not classified as QSOs.

The parameter $R = L_{[CII]}/L_{FIR}$, defined as the ratio of the [CII] line luminosity to the far-infrared continuum luminosity L_{FIR}[†] can be used to probe the strength of the ambient radiation field (G_0, e.g. Kaufman et al. 1999) under the PDR paradigm. Since the emergent FIR intensity is directly proportional to the underlying radiation field and, L$_{[CII]}$ is only weakly dependent on G_0 it follows that their ratio R is inversely proportional to G_0. Low values of R would imply a hard underlying radiation field. Despite local ULIRGs being predominantly starburst dominated (e.g. Rigopoulou et al. 1999, Farrah et al. 2007) their ratio R=$L_{[CII]}/L_{FIR}$ is surprisingly low, less than 1% (e.g. Luhman et al. 2003, Farrah et al. 2013). In contrast, high redshift ULIRGs at z$\sim$1$-$2 (e.g. Stacey et al. 2010) and z $>$ 2 lenses discovered by *Herschel* (e.g. Ivison et al 2010, Valtchanov et al. 2011) have R ratios similar to those of local star-forming galaxies.

In Fig. 2 we plot the observed R ratio as a function of L_{FIR}, for a sample of nearby normal and starburst galaxies (Malhotra et al. 2001), local ULIRGs (Farrah et al. 2013, Diaz-Santos et al. 2013), high-z star-forming and AGN-powered sources (Stacey et al. 2010), Hailey-Dunsheath et al. 2010), high-z lenses from Ivison et al (2010), Valtchanov et al. (2011), George et al. (2013) and our sample. Local star forming and normal galaxies and high-redshift star forming galaxies display ratios of $R\sim0.001-0.01$ while R is in the range $\mathbf{(1.3-10)}\times10^{-4}$ for local ULIRGs. The ratio varies between $R\approx 3\times10^{-4}-0.7\times10^{-2}$ for our sample (U)LIRGs. Turning to the two AGN sources in our sample with low $L_{[CII]}/L_{FIR}$ we note that it is plausible that a sizeable fraction of the L_{FIR} originates in the AGN component hence lowering the overall $L_{[CII]}/L_{FIR}$ ratio.

Our finding reveals, for the first time, that intermediate redshift (U)LIRGs with no AGN have $L_{[CII]}/L_{FIR}$ ratios similar to those of high-redshift star-forming galaxies and local normal galaxies. The implications of this result for the nature and evolution of ULIRGs are

[†]defined as the luminosity between 42.5$-$122.5 μm

discussed in Section 4.

3.2. The [CII]/CO(1−0) ratio and PDR properties

Early [CII] surveys of extragalactic sources and mapping of the Galaxy (e.g. Heiles et al. 1994, Cubick et al. 2008) have established that a large fraction of [CII] emission in galaxies originates in PDRs on the outer layers of molecular clouds exposed to intense far-UV radiation. [CII] also acts as a coolant of the low density warm ionized medium. Recent studies (e.g. Rigopoulou et al. 2013) found that up to 25% of the [CII] emission in the star forming galaxy IC342 originates in the diffuse ionized gas. We will thus assume that the majority of [CII] emission in our sample (U)LIRGs originates in PDRs. Kaufmann et al. (1999) presented PDR models in which the line emission from the clouds is determined by the density of the gas η and the incident flux G_0 (expressed in units of the Habing Field, $1.6\times\ 10^{-3}$ erg cm^{-2} s^{-1}). The models assume that the [CII] line and the FIR continuum are optically thin optically thick and self-absorption case is not likely (see e.g. Luhman et al. 2003) but, the low-J CO transitions are optically thick. So when comparing models to observables one needs to subtract off the fraction of the [CII] line arising in the ionized medium ($\sim$ 25%, e.g. Rigopoulou et al. 2013), and multiply the CO line intensity by a factor of two for all objects.

Using the CO measurements reported in Magdis et al. (2014) we examine the $L_{[\rm CII]}/L_{\rm CO(1-0)}$ ratio for our intermediate redshift ULIRGs. For sources without CO(1−0) measurements we use the conversion factors for submm galaxies CO(2-1)/CO(1-0) $\sim$0.84 $\pm$ 0.13 and CO(3-2)/CO(1-0) $\sim$ 0.52 $\pm$ 0.09. (e.g. Bothwell et al. 2013). The $L_{[\rm CII]}/L_{\rm CO(1-0)}$ ratio for our sample is 3300 $\pm$ 420. This value excludes the two sources that contain confirmed AGN. For comparison, local ULIRGs have a mean $L_{[\rm CII]}/L_{\rm CO(1-0)}$ ratio of 1500±260, high-z star-forming galaxies 4050±410, normal local galaxies 1800±270, while starburst nuclei and local Galactic star-forming regions have a ratio of 4100±320 (Stacey et al. 1991). We find that the mean $L_{[\rm CII]}/L_{\rm CO(1-0)}$ value for our sample is a factor of two larger than that of local ULIRGs and closer to the value found for local and high-z star-forming galaxies. Although local normal galaxies and local ULIRGs have similar $L_{[\rm CII]}/L_{\rm CO(1-0)}$ ratios, their $L_{[\rm CII]}/L_{\rm FIR}$ ratios are a factor of 10 different. Local normal galaxies have higher $L_{[\rm CII]}/L_{\rm FIR}$ values than those seen in local ULIRGs. Likewise, the $L_{[\rm CII]}/L_{\rm CO(1-0)}$ and $L_{[\rm CII]}/L_{\rm FIR}$ ratios of local and intermediate redshift ULIRGs are different by a factor of 2 and 10, reinforcing our earlier findings that the properties of the ISM of ULIRGs changes dramatically between z=0 and z=0.5.

To further investigate these trends, in Figure 3 we plot the $L_{[\rm CII]}/L_{\rm FIR}$ and $L_{\rm CO(1-0)}/L_{\rm FIR}$

ratios for our sample and compare them to those of galactic star-forming regions, local ULIRGs, local normal galaxies, high and low-z star-forming galaxies and recent *Herschel* measurements of high-z lensed star-forming galaxies from Ivison et al (2010), Valtchanov et al. (2011), and George et al. (2013). For reference, we also show PDR model calculations[‡] for gas density η and FUV strength G_0 (adapted from Hailey-Dunsheath et al 2010) applicable to sources without a dominant AGN component.

The mean $L_{[\rm CII]}/L_{\rm FIR}$ and $L_{\rm CO(1-0)}/L_{\rm FIR}$ ratios for intermediate redshift ULIRGs are a factor of 10 and 7 times higher than those of local ULIRGs. Since the emergent $L_{\rm FIR}$ is proportional to the incident radiation flux (parameterised by G_0) the smaller $L_{[\rm CII]}/L_{\rm FIR}$ line ratios observed in local ULIRGs indicate that [CII] must be produced in dense PDRs illuminated by a strong radiation field (e.g. Farrah et al. 2013). In a recent study of [CII] line emission from a sample of local ULIRGs Diaz-Santos et al. (2013) argue in favor of smaller/compact star-forming regions.

Clearly, none of the above scenarios are applicable to the intermediate redshift (U)LIRGs. The data points for our sample fall in the range $10^3 < G_0 < 10^2$ an area which overlaps with the low end of the distribution of the G_0 values for starbursts and the high end of G_0 values for normal galaxies. Hence, we conclude that the bulk of the molecular gas in intermediate redshift (U)LIRGs is exposed to a softer radiation field than that of local ULIRGs, more akin to those found in nearby starburst nuclei.

The $L_{\rm CO(1-0)}/L_{\rm FIR}$ of intermediate redshift (U)LIRGs is $\sim$7 times higher than that of local ULIRGs. It is similar to the upper end of the values seen in local starburst nuclei and local normal galaxies. However, as we discussed earlier, intermediate redshift ULIRGs display an $L_{[\rm CII]}/L_{\rm CO(1-0)}$ ratio of 3000 which is higher than the value found in local normal galaxies but lower that that of starburst nuclei (4100). A lower $L_{[\rm CII]}/L_{\rm CO(1-0)}$ (for the same $L_{\rm CO(1-0)}/L_{\rm FIR}$ value) ratio would imply that most of the CO emission originates in molecular clouds residing in less active star-forming regions than those responsible for producing the fine-structure emission lines.

4. The Nature and Evolution of Luminous Infrared Galaxies

The star formation rate density (SFRD) in the Universe increases dramatically from the present day to $z\sim1$ at which point it becomes flat out to $z\sim3-4$ (e.g. Bouwens et al. 2009, Magnelli et al. 2013). Luminous Infrared Galaxies are a dominant component to the

[‡]based on PDRToolbox (PDRT) web site: http://dustem.astro.umd.edu/)

co-moving SFRD between $z{\sim}0.5{-}1$ so their properties may give clues to the drivers behind the dramatic rise at $z{<}1$.

Although local ULIRGs have been used as templates for $z{\sim}2$ luminous infrared galaxies, increasing evidence exists (e.g. Papovich et al. 2007, Farrah et al. 2008, Swinbank et al. 2010) that they are distinctly different to their high-z counterparts.

It is now well established that the intense star-forming activity of local ULIRGs is the result of merging (e.g. Sanders & Mirabel 1999). Morphology indications in high-resolution *HST* images however, reveal that, at $z{\sim}2$ at least 50% of the Herschel-selected starbursts are not driven by galaxy mergers (e.g. Kartaltepe et al. 2011). In section 3 we presented new evidence that the properties of the star-forming regions of our intermediate redshift (U)LIRGs are distinctly different to those of local ULIRGs. Instead, they bear a closer resemblance to those found in high redshift star-forming galaxies. In particular, we found evidence that the star-forming regions of our $z{\sim}0.5$ (U)LIRGs are illuminated by moderately intense FUV radiation, with G_0 in the range $10^2{-}10^{2.5}$ and G_0/η $\sim$0.1$-$1 cm^3 (when the appropriate corrections of $0.7{\times}L_{\rm [CII]}$ and $2{\times}L_{\rm CO}$ are applied). Similar G_0/η values have been found for local normal and starburst galaxies (e.g. Wolfire et al. 1990). In contrast, the low $L_{\rm [CII]}/L_{\rm FIR}$ values seen in local ULIRGs are the result of the presence of intense radiation fields G_0 with high column densities $G_0/\eta \sim 0.02{-}0.03$ cm^3 (Farrah et al. 2013) and possibly compact sizes (e.g. Diaz-Santos et al. 2013). The high $L_{\rm [CII]}/L_{\rm FIR}$ values seen in intermediate redshift ULIRGs together with the modest radiation fields speak against the existence of such dense compact PDRs, hence the star-forming regions of intermediate redshift (U)LIRGs must be extended.

Our survey has revealed a strong evolution in the properties of ULIRGs at $0.2{<}z{<}0.8$ and confirms the use of the [CII] line and the $L_{\rm [CII]}/L_{\rm IR}$ and $L_{\rm C[II]}/L_{\rm CO(1-0)}$ ratios, in probing the properties of the star forming regions in galaxies at low, intermediate and high redshifts. Even at modest redshifts ($z{\sim}0.5$) the nature of the ULIRG population changes significantly from exclusively compact merger-driven to a more varied population.

We thank the anonymous referee for his/her insightful comments. DR and GEM acknowledge support from grant ST/K00106X/1 and the John Fell Oxford University Press (OUP) Research Fund (GEM). This paper is based on data from *Herschel's* SPIRE-FTS. SPIRE has been developed by a consortium of institutes led by Cardiff Univ. (UK) and including: Univ. Lethbridge (Canada); NAOC (China); CEA, LAM (France); IFSI, Univ. Padua (Italy); IAC (Spain); Stockholm Observatory (Sweden); Imperial College London, RAL, UCL-MSSL, UKATC, Univ. Sussex (UK); and Caltech, JPL, NHSC, Univ. Colorado (USA). This development has been supported by national funding agencies: CSA (Canada);

NAOC (China); CEA, CNES, CNRS (France); ASI (Italy); MCINN (Spain); SNSB (Sweden); STFC, UKSA (UK); and NASA (USA).

Facilities: Herschel, IRAM:30m, APEX.

REFERENCES

Blain, A.W., Smail, I., Ivison, R.J., Kneib, J-P., Frayer, D.T. 2002, PhR, 369, 111

Bouwens, R. J., Illingworth, G. D., Franx, M., et al. 2009, ApJ, 705, 936

Crawford, M.K., Genzel, R., Townes, C.H., Watson, D.M. 1985, ApJ, 291, 755

Cubick, M., Stutzki, J., Ossenkopf, V., Kramer, C., Rollig, M. 2008, A&A, 488, 623

Diaz-Santos, T., Armus, L., Charmandaris, V., et al. 2013, ApJ, 774, 68

Farrah, D., Lonsdale, C. J., Weedman, D. W., et al. 2008, ApJ, 677, 957

Farrah, D., Lebouteiller, V., Spoon, H., et al. 2013, ApJ, in press

Fu, H., Cooray, A., Feruglio, C., et al. 2013, Nature, 498, 338

Fulton, T., Hopwood, R., Baluteau, J.-P. 2013, in preparation

Genzel, R., Lutz, D., Sturm, E., et al. 1998, ApJ, 498, 579

George, R.D., Ivison, R. J., Hopwood, R., et al. 2013, MNRAS, in press

Gracia-Carpio, J., Sturm, E., Hailey-Dunsheath, S. et al. 2010, ApJ, 728, 7

Hailey-Dunsheath, S., Nikola, T., Stacey, G. J. 2010, ApJ, 714, 162

Heiles, C., 1994 ApJ, 436, 702

Ivison, R. J., Swinbank, A. M., Swinyard, B.M, et al. 2010, A&A, 518, 35

Kaufman, M.J., Wolfire, M. G., Hollenbach, D. J., Luhman, M. 1999, ApJ, 527, 795

Lagache, G., Puget, J-L., Dole, H. 2005, ARA&A, 43, 727

Le Floc'h, E., Papovich, C., Dole, H., et al. 2005, ApJ, 632, 169

Luhman, M.L., Satyapal, S., Fischer, J., et al. 1998, ApJ, 504, L11

Magnelli, B., Poppeso, P., Berta, S., et al. 2013, A&A, 553, 112

Malhotra, S., Kaufman, M. J., Hollenbach, D., et al. 2001, ApJ, 561, 766

Muzzin, A., van Dokkum, P., Kriek, M., et al. 2010, ApJ, 725, 742

Oliver, S.J., Bock, J., Altieri, B., et al. 2012, MNRAS, 424, 1614

Ott, S. 2010, ASP Conference Series, 434, 139

Papovich, C., Rudnick, G., Le Floc'h, E., et al. 2007, ApJ, 668, 45

Pilbratt, G.L, Riedinger, J. R., Passvogel, T., et al. 2010, A&A, 518, 1

Rigopoulou, D., Spoon, H. W. W., Genzel, R., et al. 1999, AJ, 118, 2625

Rigopoulou, D., Hurley, P., Swinyard, B.M. 2013, MNRAS, 434, 2015

Rodighiero, G., Cimatti, A., Gruppioni, C., et al. 2010, ApJ, 518, 25

Rujopakarn, W., Rieke, G.H., Eisenstein, D.J., Juneau, S. 2011, ApJ, 726, 93

Stacey, G. J., Geis, N., Genzel, R., et al. 1991, ApJ, 373, 423

Stacey, G.J., Hailey-Dunsheath, S., Ferkinhoff, C., et al. 2010, ApJ, 724, 957

Swinbank, A. M., Smail, I., Chapman, S. C., et al. 2010, ApJ, 405, 234

Valtchanov, I.,Virdee, J., Ivison, R. J., et al. 2011, MNRAS, 415, 3473

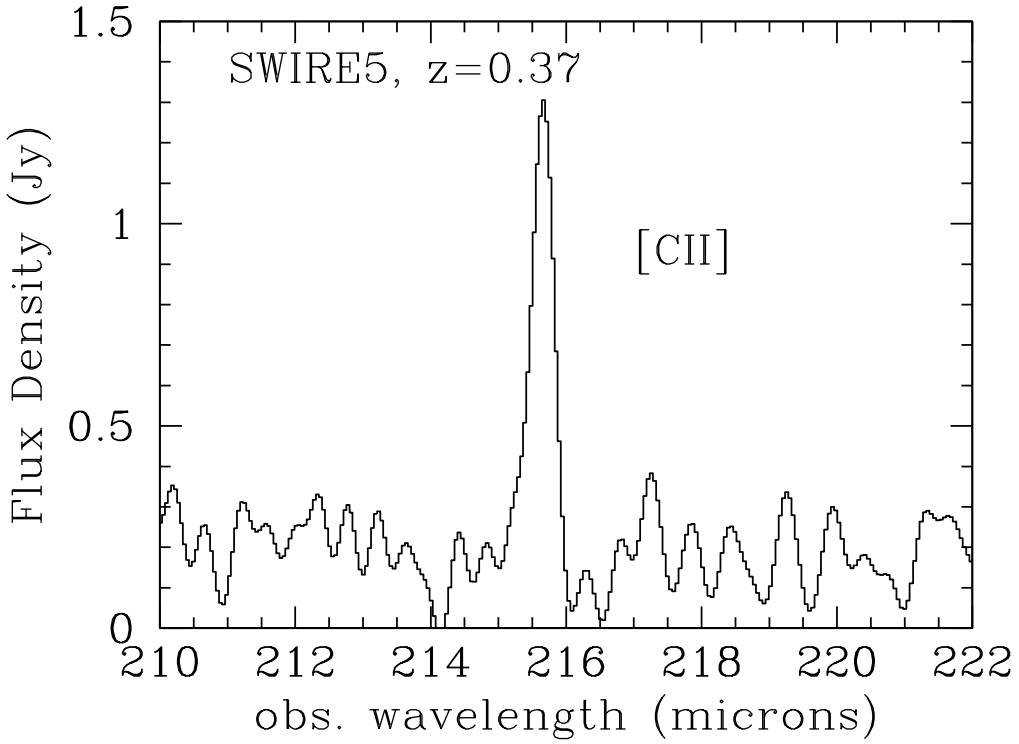

Fig. 1.— Continuum-subtracted region of the FTS spectrum around the [CII] line in the observed frame for one of our sample ULIRGs (SWIRE5) at z=0.37.

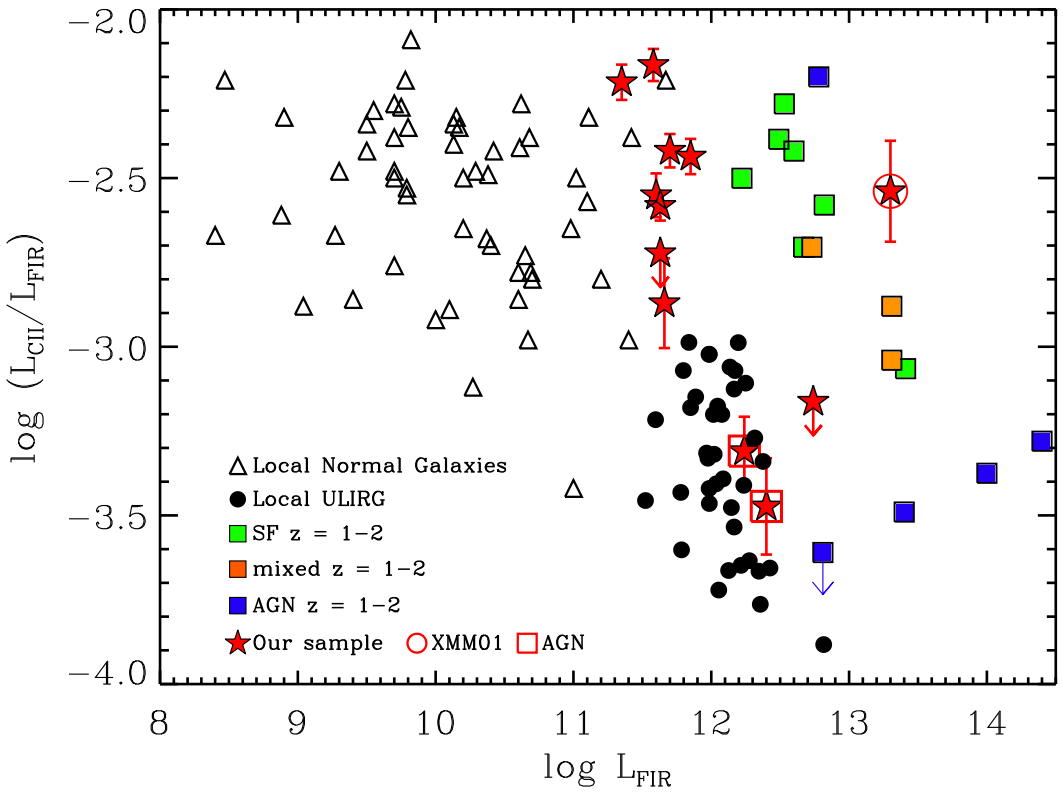

Fig. 2.— Log($L_{[\mathrm{CII}]}/L_{\mathrm{FIR}}$) as a function of log($L_{\mathrm{FIR}}$) for local normal and starburst galaxies (open triangles) from Malhotra et al. (2001), local ULIRGs (black filled circles) from Farrah et al. (2013) and Diaz-Santos et al. (2013), high-redshift ($1 < z < 2$) star-forming galaxies (green squares), mixed systems (orange filled squares) and AGN (blue filled squares) from Stacey et al. (2010). Red stars denote the 12 intermediate redshift (U)LIRGs presented in this work (circled star is XMM01, squared stars denote AGN). Note that $L_{\mathrm{FIR}(42.5-122.5\,\mu\mathrm{m})} = 0.63 \times L_{\mathrm{IR}(8-1000\mu\mathrm{m})}$.

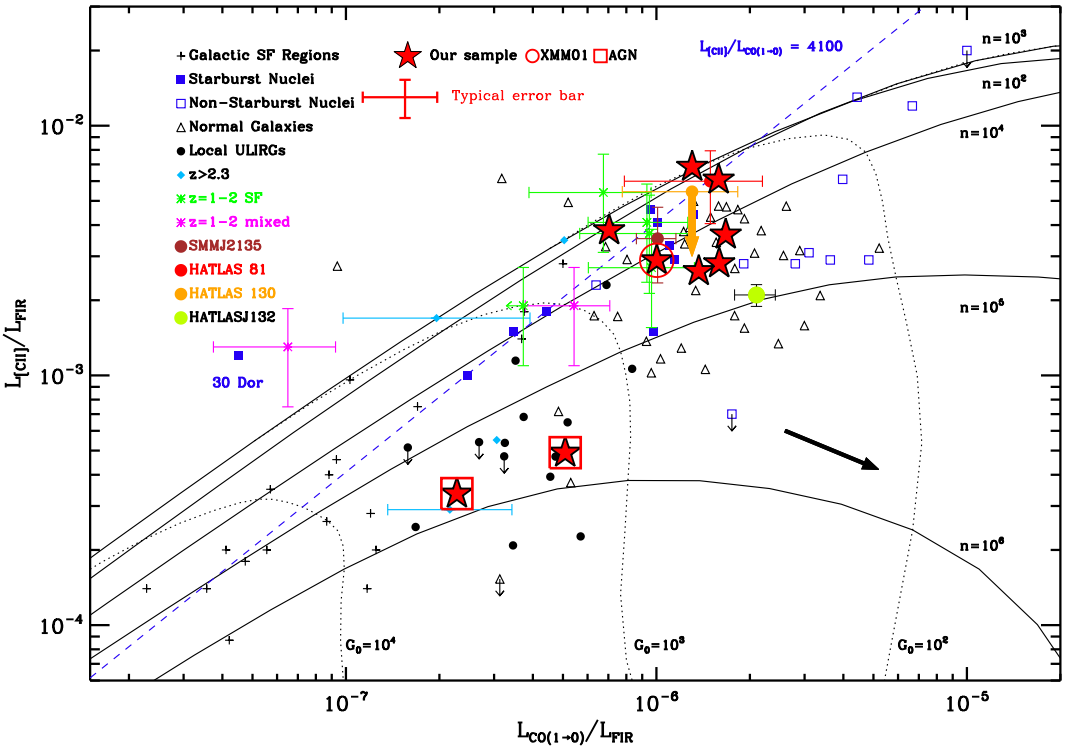

Fig. 3.— $L_{[\mathrm{CII}]}/L_{\mathrm{FIR}}$ as a function of $L_{\mathrm{CO}(1-0)}/L_{\mathrm{FIR}}$ for Galactic star-forming regions (crosses), local starburst nuclei (filled squares), local non-starburst nuclei (open squares), local normal galaxies (triangles), local ULIRGs (circles), redshift 1 to 2 sources (asterisks with error bars), high z sources (cyan diamonds), adapted from Hailey-Dunsheath et al. (2010). Herschel lenses are from: SMMJ2135 (Ivison et al. 2010), HATLAS 81 & HATLAS 130 (Valtchanov et al. 2011), HATLASJ132 (George et al. 2013). Red asterisks denote the present sample (circled star is XMM01, squared stars denote AGN). The typical error bar shown refers to our sample only. Overplotted are the PDR model values for η and G_0 from Kaufmann et al. (1999). The plot is based on observed values and is intended as a first order diagnostic tool, hence does not include any correction. The black arrow indicates the direction that all data points in the plot will shift when corrections are applied (see text).